Digital Signal Processing 21 (2011) 131–140

Contents lists available at ScienceDirect

Digital Signal Processing

www.elsevier.com/locate/dsp

Optimization approach to adapt Kalman filters for the real-time application of accelerometer and gyroscope signals' filtering

Cezary Kownacki

Faculty of Mechanical Engineering, Technical University of Bialystok, ul. Wiejska 45C, 15-351 Bialystok, Poland

ARTICLE INFO

Article history:
Available online 7 September 2010

Keywords:
Strapdown system
Accelerometer
Gyroscope
Acceleration
Angular rate
Signal filtering
Discrete Kalman filter
Optimization
Process noise covariance matrix
Measurement noise covariance matrix

ABSTRACT

A problem of accelerometer and gyroscope signals' filtering is discussed in the paper. Triple-axis accelerometer and three single-axis gyroscopes are the elements of strapdown system measuring head. Effective noise filtration impacts on measured signal reliability and the computation precision of moving object position and orientation. The investigations were carried out to apply Kalman filter in a real-time application of acceleration and angular rate signals filtering. The filter parameter adjusting is the most important task of the investigation, because of unknown accuracy of the measuring head and unavailability of precisely known model of the system and the measurement. Results of calculations presented in the paper describe relation between filter parameters and two assumed criterions of filtering quality: output signal noise level and filter response rate. The aim of investigation was to achieve and find values of the parameters which make Kalman filter useful in the real-time application of acceleration and angular rate signals filtering.

1. Introduction

Technical progress of IC (Integrated Circuits) sensors' and microprocessors' systems results in replacement of a traditional platform system (inertial navigation system based on gimbals) by a strapdown system with rigidly mounted accelerometers and gyroscopes to the fuselage of the moving object. The main advantages of strapdown systems with IC sensors are its small overall dimensions and weight, so it is possible to mount it into objects, where there is not enough available space for the platform system, i.e. in a mobile robot or in a robot manipulator clutch. The strapdown system has also simpler and rigid structure insensitive to shocks and vibrations. Lack of gimbals, slip rings, and bearings leads to lower cost and higher reliability of the strapdown system. However, the strapdown system requires precise sensor calibration and alignment, and also high precision of calculations, which depends on reliable measurement of acceleration and angular rate signals [1–3].

Sensor bias errors, inertial errors, motion-inducted errors and any random noise are accumulated due to iterative routine of coordinate transformation and yaw, pitch and roll angles computation. Therefore one of important aspects of the strapdown system reliability is a real-time signal filtering [4,2,3].

The easiest way to perform signal filtering is the application of a low-pass filter. But low-pass filters can be used only for noise cancelation with known a priori bandwidth, e.g. from signal spectral analysis. Acceleration and angular rate signals describe a random process of object movement, so not all of noise sources and its bandwidths can be identified in a laboratory. Kalman filter seems to be more suitable, because it estimates useful signal basing on the knowledge about the system, behavior in the real world. The system behavior is described by the state-space representation and uncertainties in the system namely the measurement noise and the process noise [5]. Usually the first uncertainty can be identified, because

E-mail address: cezarkw@poczta.onet.pl.

1051-2004/$ – see front matter
doi:10.1016/j.dsp.2010.09.001

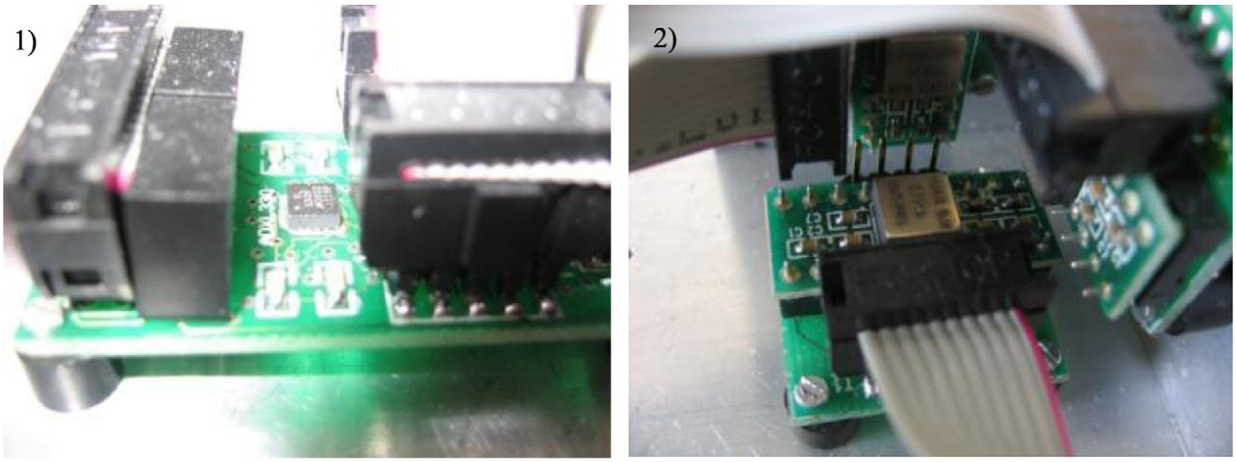

Fig. 1. Electronic circuits and IC sensors of acceleration and angular rate: 1) ADXL330 triple-axis accelerometer, 2) ADXRS300 single-axis gyroscope.

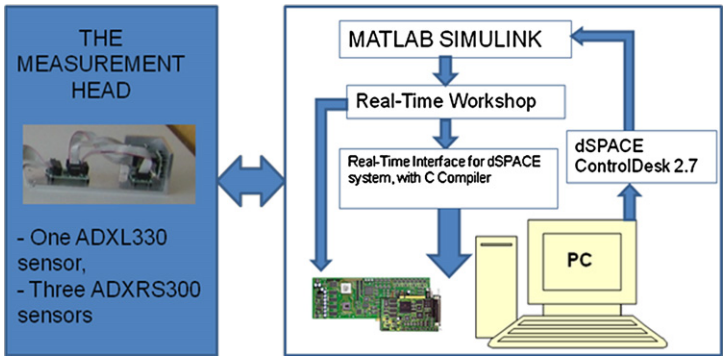

Fig. 2. The diagram of research station.

accuracy of many measurement instruments is available. So the measurement noise covariance matrix characterizing the measurement accuracy is also known a priori [6–8].

The problem is how to adjust Kalman filter if there is no information about the accuracy of measurement instrument and there is no possibility to determine precise model of the system and the measurement [9]. It happens when the measurement instrument is a completely new designed and built device such as the measuring head of strapdown system presented in the paper. So, we carried out the research to adjust Kalman (KF) filter parameters for a real-time application of acceleration and angular rate signals filtering. The results are surprising, because values of optimal KF parameters ensuring the best signal filtration are outside the range 0–1 usual for a covariance.

2. The measuring head and apparatus

The measuring head was designed and built for the research into the strapdown system navigation algorithms. The measuring head contains four sensors: one triple-axis ADXL330 accelerometer (full range-scale ± 3 g) and three single-axis ADXRS300 gyroscopes (full range-scale $\pm 300°/s$) (Fig. 1).

All of them are single chip sensors. In future the measuring head will be extended by an electronic compass, e.g. HMC6052. Acceleration and angular rate signals are transferred from the measuring head to a personal computer using dSPACE DS1005 DSP system equipped in multichannel 16 bit AD converter board DS2002. The research station and all of measurement apparatus and software engaged in the investigation are shown as a diagram in Fig. 2.

Electronic circuits of ADXL330 and ADXRS300 sensors contain capacitors at every signal output fulfilling the role of low-pass filter. The desired bandwidth can be selected by choosing of a right capacitance value. The equation for 3 dB bandwidth of ADXL330 accelerometer is as follows [10]:

$$F_{-3\ \mathrm{dB}} = 1/\left(2\pi\,(R_{FILT} = 32\ \mathrm{k\Omega}) \times C_{(X,Y,Z)}\right) \tag{1}$$

where $C_{(X,Y,Z)}$ is capacitor at corresponding X-, Y-, or Z-axis output.

The resistor R_{FILT} (32 [kΩ]) has the tolerance varying in the range $\pm 15\%$ of its nominal value, therefore the bandwidth can also be varied accordingly. We have selected capacitance of 0.1 [μF] for C_X, C_Y, and C_Z capacitors, thus according to (1)

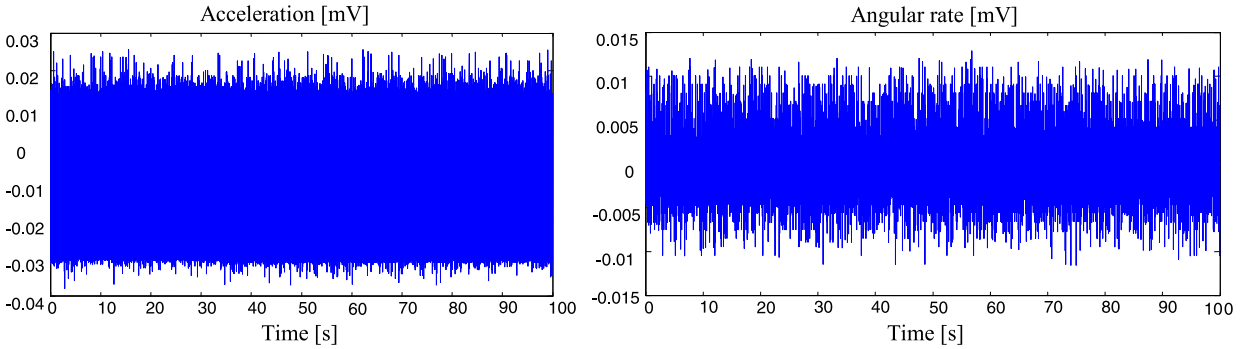

Fig. 3. Centered signals of: 1) acceleration, 2) angular rate, for the motionless measuring head.

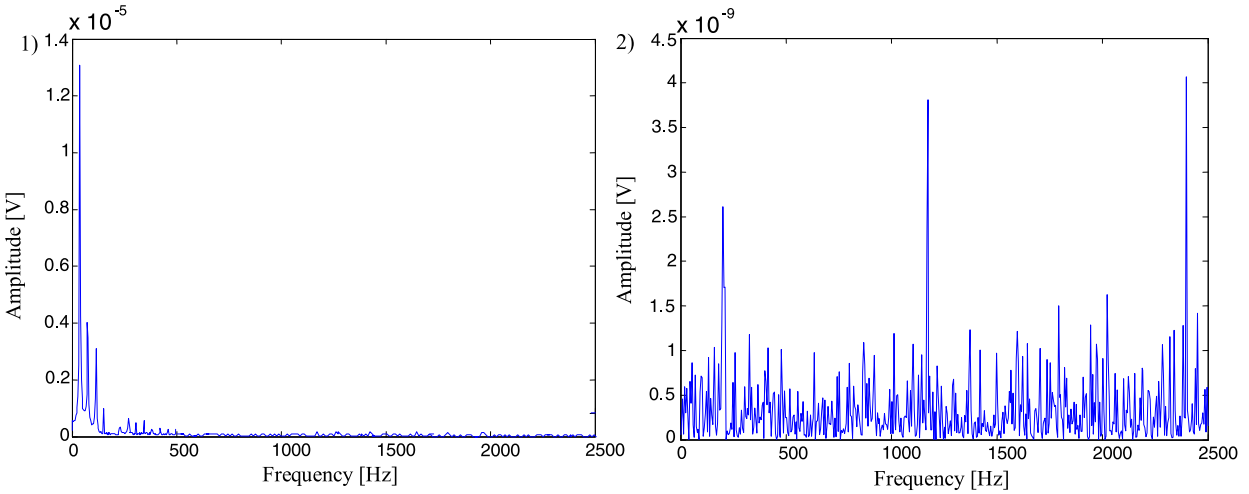

Fig. 4. The result of spectral analysis: 1) Welch spectra of the acceleration signal, 2) Welch spectra of the angular rate signal.

the bandwidth is 50 [Hz]. We assumed that the noise of ADXL330 accelerometer is a white Gaussian noise proportional to the square root of the bandwidth according to the sensor data sheet [10].

The equation for 3 dB bandwidth of ADXRS300 gyroscope is the same as Eq. (1), but the value of resistor R_{FILT} can be modified by application an external resistor between RATEOUT and SUMJ pins. The equation for resultant resistance of R_{FILT} is as follows [11]:

$$R_{OUT} = 180\ \text{k}\Omega \times R_{EXT}/180\ \text{k}\Omega + R_{EXT}. \tag{2}$$

The external resistor was not used so the resistance of R_{OUT} equals the nominal value of on-chip resistor, i.e. $180 \pm 1\%$ [kΩ], while the capacitance of 22 [nF] was selected for C_{OUT} (the capacitor at rate output). Thus the bandwidth of ADXRS300 is limited to 40 [Hz]. There is another low-pass filter in the gyroscope circuit – a capacitor at CIMD pin. Its primary purpose is to limit the high frequency demodulation artifacts before final amplification [11].

In spite of the fact that all sensors have low-pass filters built in the electronic circuit, output signals are still noised (Fig. 3). Probably the noise is generated in the circuit behind capacitors, somewhere between the measuring head and the AD converter board. Spectral analysis of output signals received from the motionless measuring head is presented in Fig. 4.

Spectral analysis of both signals: acceleration and angular rate indicates the necessity of additional signal filtering. The acceleration signal contains harmonic components with frequencies in the range from 50 [Hz] to 500 [Hz]. In turn the angular rate signal contains noise having characteristics similar to a white Gaussian noise. So we carried out the investigation to prepare KF for the real-time filtering application using DSP system.

3. Kalman filter (KF) design

Kalman filter is a discrete estimator of state-space variables of continuous dynamical system. It is commonly used for filtering and conditioning of the signals in navigation systems [12–15,6–8]. Kalman filter (KF) eliminates random noises and errors using the knowledge about the state-space representation of system and uncertainties in the process: the measurement noise and the process noise. So it is very useful as a signal filter in case of signals with random disturbances or when signal errors can be treated as an additional state-space variable in the system [12,5,15].

The general state-space representation of a linear time-invariant single-input–single-output continuous system has the form [5,15]:

$$\dot{X}(t) = F \cdot X(t) + B \cdot \big[u(t) + w(t)\big], \qquad z(t) = C \cdot X(t) + v(t), \tag{3}$$

where:

$X(t)$ – the state vector at the time t,
$u(t)$ – the control signal vector (system input) at the time t,
$z(t)$ – the system output (measured signal) at the time t,
$w(t)$ – the process noise at the time t,
$v(t)$ – the measurement noise at the time t,
F, B, C – matrices of the state-space representation: F – the state $(n \times n)$, B – the input $(n \times n)$, C – the output $(1 \times n)$.

Above equations for the equivalent discrete system are given by formulas:

$$X_{k+1} = \Phi \cdot X_k + G \cdot [u_k + w_k], \qquad z_{k+1} = H \cdot X_{k+1} + v_{k+1}, \tag{4}$$

where:

X_k – the state vector at time k,
u_k – the control signal vector (system input) at time k,
z_k – the system output (measured signal) at time k,
w_k – the process noise at time k,
v_k – the measurement noise at time k,
Φ, G, H – matrices of the state-space representation: F – the state $(n \times n)$, G – the input $(n \times n)$, H – the output $(1 \times n)$.

Matrixes of the discrete system can be calculated from following equations as a result of the first approximation [5,15]:

$$\Phi \approx I + T \cdot F, \qquad G \approx T \cdot B, \qquad H = C, \tag{5}$$

where:

T – the sample time,
F, B, C – matrixes of the state-space representation of the continuous system,
Φ, G, H – matrixes of the state-space representation of the discrete system.

Two variables v_{k+1} and w_k in Eqs. (4) are discrete white Gaussian noises with the expected value equal zero, known distributions and uncorrelated to each other [5,15].

$$E(v_k) = 0, \qquad E(w_k) = 0, \qquad E\big(v_k \cdot v_k^T\big) = R_k, \qquad E\big(w_k \cdot w_k^T\big) = Q_k, \tag{6}$$

where:

R_k – the covariance matrix of the measurement noise v_k,
Q_k – the covariance matrix of the process noise w_k,
$E[\xi]$ – the expected value of ξ,
w_k – the process noise at time k,
v_k – the measurement noise at time k.

Uncertainties in the system described by v_k and w_k are named accordingly the measurement noise and the process noise. Eqs. (3) and (4) assume that matrixes B and G decide about the position of both control signal u_k and the process noise w_k in the state-space equations' system.

The following model of Kalman filter was applied in our case [5,15]:

$$\hat{x}_{k+1|k} = \Phi \cdot \hat{x}_{k|k}, \qquad P_{k+1|k} = \Phi \cdot P_{k|k} \cdot \Phi^T + G \cdot Q_k \cdot G^T, \qquad K_{k+1} = P_{k+1|k} \cdot H^T \cdot \big(H \cdot P_{k+1|k} \cdot H^T + R_{k+1}\big)^{-1},$$
$$\hat{x}_{k+1|k+1} = \hat{x}_{k+1|k} + K_{k+1} \cdot (z_{k+1} - H \cdot \hat{x}_{k+1|k}), \qquad P_{k+1|k+1} = (I - K_{k+1} \cdot H) \cdot P_{k+1|k}, \tag{7}$$

where:

$\hat{x}_{k|k}$ – the state estimate at time k,
$\hat{x}_{k+1|k}$ – the predicted state,
$P_{k|k}$ – the error covariance matrix at time k,

$P_{k+1|k}$ – the predicted error covariance matrix,
Φ, G, H – matrixes of the state-space representation of the discrete system,
K_{k+1} – the gain vector at time $k+1$,
z_{k+1} – the measured signal (system output),
Q_k – the covariance matrix of the process noise w_k at time k,
R_{k+1} – the covariance matrix of the measurement noise v_k at time $k+1$.

The first step in the design of Kalman filter for a considered application is to determine the mathematical model describing system behavior in the real world. In case of the measurement of the acceleration and the angular rate it is difficult to identify any deterministic disturbance or control signal, because the motion tracked with the strapdown system is a typical random process. Thus the model of KF is a simplified version of KF for systems with omitted control signal u_k [5]. We assumed that acceleration is constant, equals zero, or varies very slowly. So the state-space representation (3) for the acceleration a is given by:

$$\dot{X}(t) = \frac{d}{dt}\begin{bmatrix} V \\ \dot{V} \end{bmatrix} = \begin{bmatrix} 0 & 1 \\ 0 & 0 \end{bmatrix} \cdot X(t) + \begin{bmatrix} 1 & 0 \\ 0 & 1 \end{bmatrix} \cdot w(t) = F \cdot X(t) + B_A \cdot w(t),$$
$$Z(t) = [0 \quad 1] \cdot X(t) + v(t) = C_A \cdot X(t) + v(t), \qquad X(t) = \begin{bmatrix} V \\ a \end{bmatrix}, \tag{8}$$

where:

V – the linear rate,
a – the acceleration,
F, B_A, C_A – matrixes of the state-space model.

Similarly we assumed that angular rate is constant or varies uniformly. Thus, the state-space representation (3) for the angular rate is as follows:

$$\dot{X}(t) = \frac{d}{dt}\begin{bmatrix} \omega \\ \dot{\omega} \end{bmatrix} = \begin{bmatrix} 0 & 1 \\ 0 & 0 \end{bmatrix} \cdot X(t) + \begin{bmatrix} 1 & 0 \\ 0 & 1 \end{bmatrix} \cdot w(t) = F \cdot X(t) + B_G \cdot w(t),$$
$$Z(t) = [1 \quad 0] \cdot X(t) + v(t) = C_G \cdot X(t) + v(t), \qquad X(t) = \begin{bmatrix} \omega \\ \varepsilon \end{bmatrix}, \tag{9}$$

where:

ω – the angular rate,
ε – the angular acceleration,
F, B_G, C_G – matrixes of the state-space model.

Eqs. (8) and (9) have different matrixes C and B which were indicated by different letters in bottom index (C_G, B_G – the angular rate, C_A, B_A – the acceleration). The system matrix F is the same for both.

Next, a Simulink model of Kalman filter (7) was built for linear time-invariant single-input–single-output continuous system (3). The control signal vector u_k was omitted in the model and the rank of the system matrix A is constant and it equals 2. Only elements of F, B, and C matrixes are variant parameters of the Simulink model, which should be set accordingly to the state-space representation of system (8) or (9) considered at the moment. In the last step of the investigation we have adjusted KF parameters, i.e. the covariance matrix R_k (1×1) of the measurement noise, the covariance matrix Q_k (1×1) of the process noise and the error covariance matrix P_0 (2×2) at time $k = 0$.

4. Adjusting of KF parameters

At the beginning we analyzed and filtrated signals recorded for the motionless measuring head, hoping it would help in the identification of both the measurement noise and the process noise. So the right values of covariance matrixes R_k, Q_k, and P_0 would be also available, though the measurement accuracy of the measuring head is unknown. Two filters: high-pass and low-pass were applied to identify the measurement noise and the process noise. The cut-off frequency between stop-band and pass-band for both filters is the same and it equals 1 [Hz]. The frequency was set intuitively because there are no indicators telling how to identify bandwidth of the process noise and the measurement noise. It was assumed that the process noise bandwidth is located at range of lower frequencies, probably the same as the bandwidth of the real signal of acceleration or angular rate. In turn the bandwidth of the measurement noise should be at higher frequency range than the process noise bandwidth. So the high-pass filter stops the process noise and vice versa the low-pass filter stops the measurement noise. Hence, values of R_k and Q_k covariance were evaluated separately for accelerometer and gyroscope (Table 1).

Table 1
Values of R_k and Q_k covariances computed from accelerometer and gyroscope signals.

	Accelerometer ADXL330	Gyroscope ADXRS300
R_k	1.8472×10^{-4}	1.3872×10^{-6}
Q_k	1.1859×10^{-8}	2.4907×10^{-9}

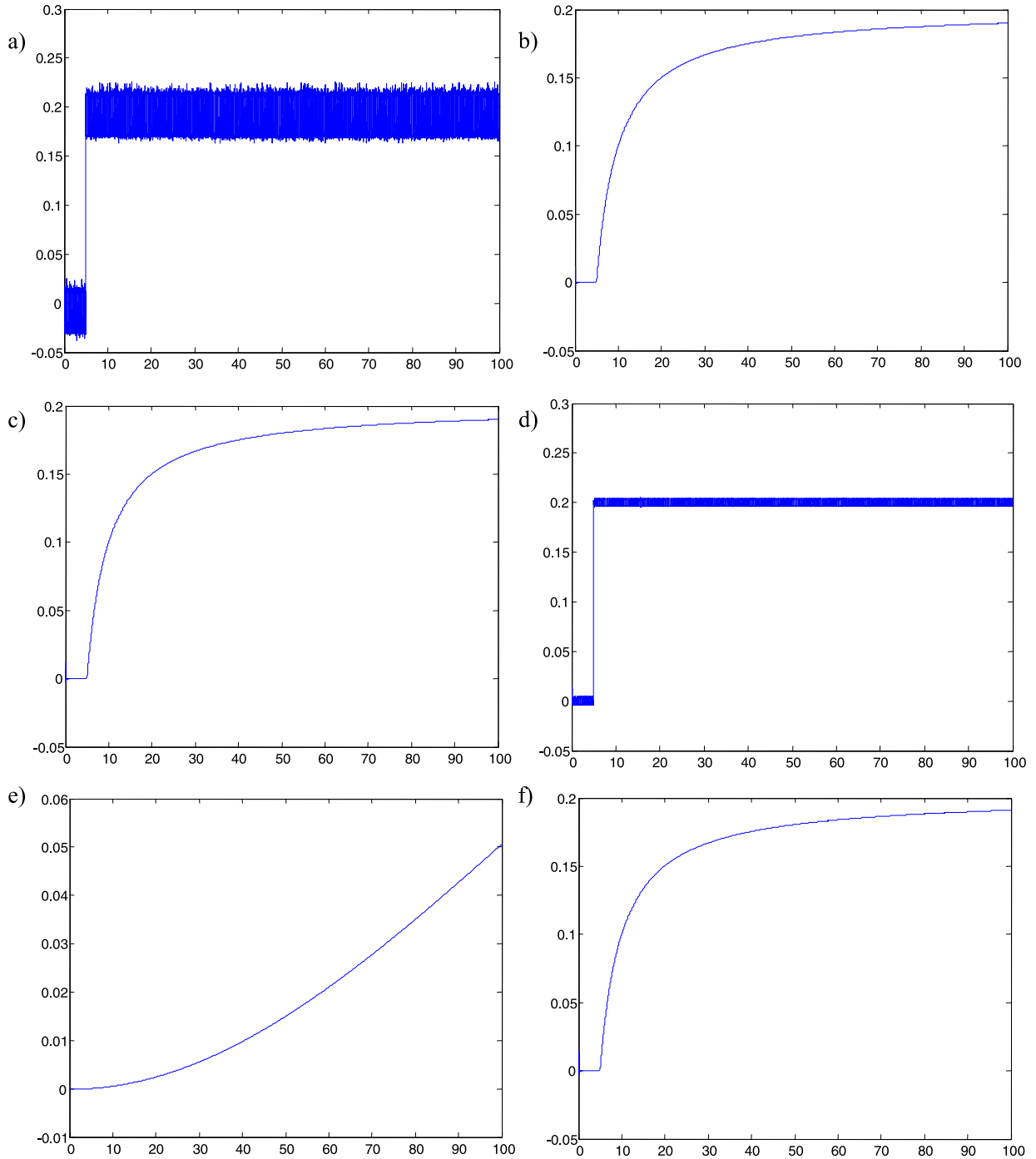

Fig. 5. The filtered acceleration signal behavior for different values of R_k, Q_k, and P_0. The input signal was a sum of the step signal and acceleration signal: a) $R_k = 0$, $Q_k = 1.1859 \times 10^{-8}$, $P_0 = [11; 11]$; b) $R_k = 1$, $Q_k = 1.1859 \times 10^{-8}$, $P_0 = [11; 11]$; c) $R_k = 1.8472 \times 10^{-4}$, $Q_k = 0$, $P_0 = [11; 11]$; d) $R_k = 1.8472 \times 10^{-4}$, $Q_k = 1$, $P_0 = [11; 11]$; e) $R_k = 1.8472 \times 10^{-4}$, $Q_k = 1.1859 \times 10^{-8}$, $P_0 = [00; 00]$; f) $R_k = 1.8472 \times 10^{-4}$, $Q_k = 1.1859 \times 10^{-8}$, $P_0 = [11; 11]$.

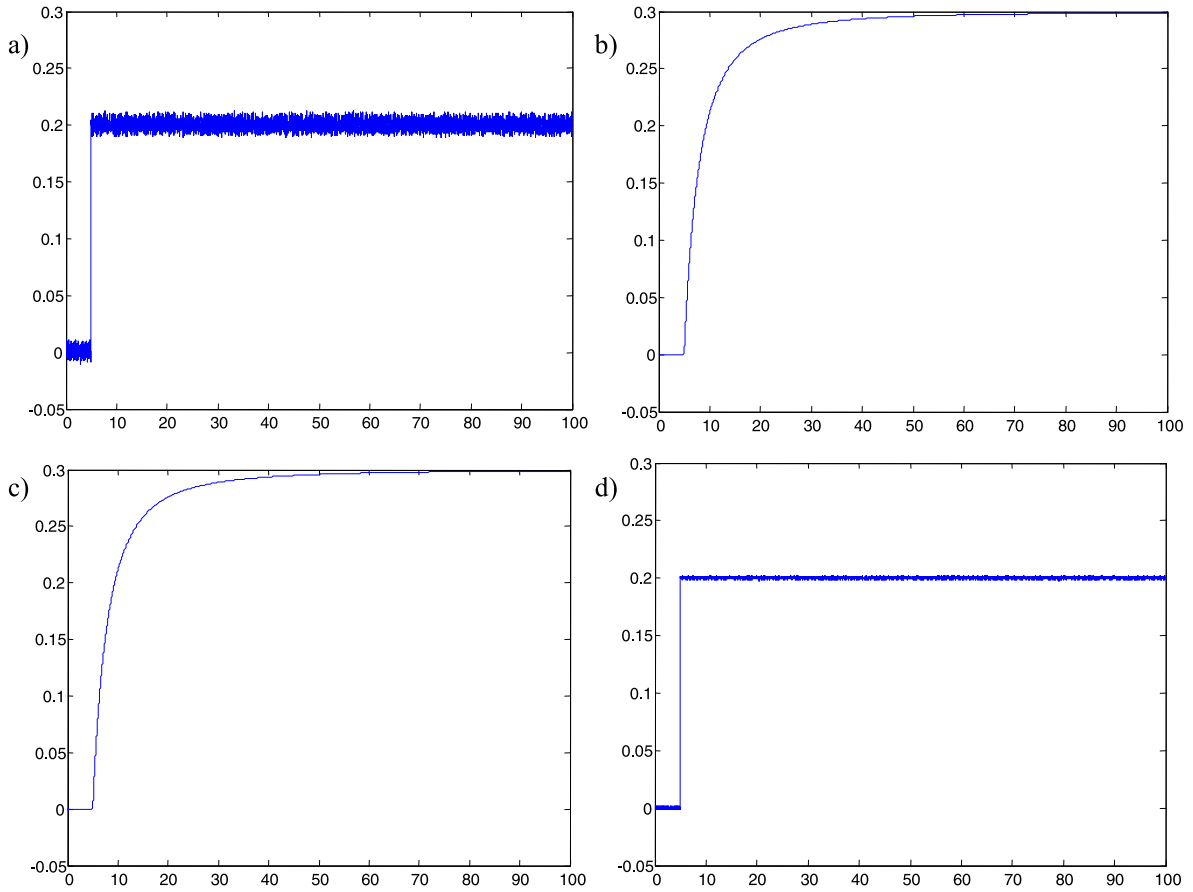

Fig. 6. The filtered angular rate signal behavior for different values of R_k, Q_k. The input signal was a sum of the step signal and angular rate signal: a) $R_k = 0$, $Q_k = 2.4907 \times 10^{-9}$, $P_0 = [11; 11]$; b) $R_k = 1$, $Q_k = 2.4907 \times 10^{-9}$, $P_0 = [11; 11]$; c) $R_k = 1.3872 \times 10^{-6}$, $Q_k = 0$, $P_0 = [11; 11]$; d) $R_k = 1.3872 \times 10^{-6}$, $Q_k = 1$, $P_0 = [11; 11]$.

Above values of R_k and Q_k were computed for centered signals, i.e. with the mean value equals zero. Values of P_0 matrix elements define initial condition of KF, so they impact only on a KF start-up. The result of offline filtering using parameters' values from Table 1 seems to be perfect, because all noises were cancelled and all output signals for the motionless measuring head were almost constant. But the question is how the designed KFs behave during a real-time operation. So the desired application for DSP system was prepared and it shows that designed KFs response rate is too low. The observed lag of filtered signals of acceleration and angular rate is unacceptable for any application of designed KFs. We decided to test how KF works depending on values of R_k, Q_k, and P_0.

The aim of the test was to observe the KF behavior for different values of single parameter simultaneously having remaining parameters constant. A sum of the step signal and measured signals of acceleration or angular rate was used as the input signal of the KF in the test. Some test results are presented in Figs. 5 and 6.

It is no doubt the KF parameters R_k, Q_k, and P_0 impact not only on the noise level of output signal, but also on the inertia of KF response. The inversely proportional relation between the inertia and the noise level is clearly shown in Figs. 5 and 6. The inertia increases together with value of R_k while the noise level decreases. And conversely, the inertia decreases with the increase of value of Q_k, while the noise level increases. The sensor noise covariance R_k has stronger influence on the noise level among both of covariance matrixes R_k and Q_k (Figs. 6a and 6d). However, the matrix P_0 only modifies the lag at time $k = 0$ and its elements equal 1 assure the best KF dynamics for acceleration and angular rate signals filtering.

Although an appreciable knowledge about KFs behavior is available from literature and the test, the problem of adjusting KF parameters for the real-time filtering application is still unsolved. Because of that we have decided to use an optimization method and to formulate a cost function which is minimized for optimal KF parameters satisfying both conditions of the lowest noise level and the lowest inertia. The function is given by equation:

$$I(R_k, Q_k) = \int_{t=t_s}^{t_f} \left(S(\tau) - \hat{x}(\tau, R_k, Q_k)\right)^2 d\tau + \int_{f=0}^{f=\frac{F_s}{2}} \left|\left(\hat{X}(f, R_k, Q_k)\right)\right| df, \tag{10}$$

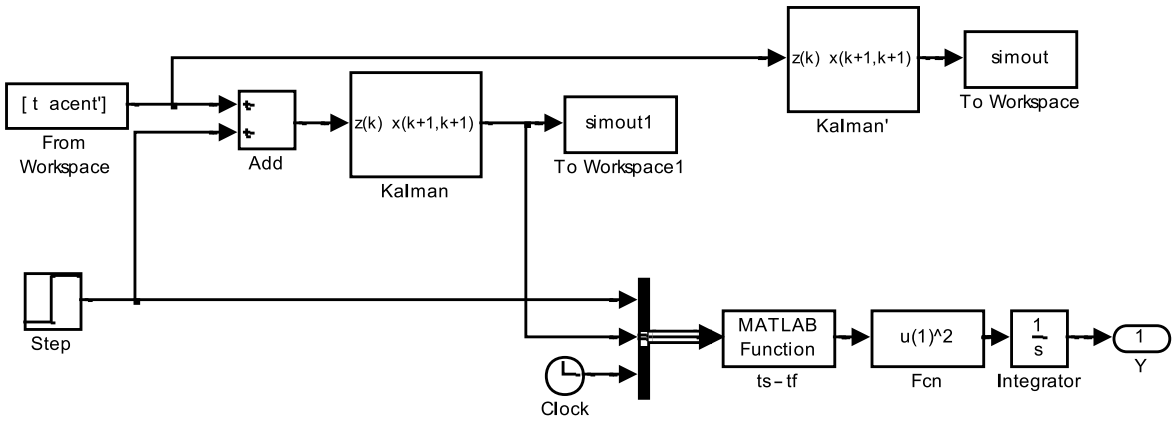

Fig. 7. The Simulink model calculating the first integral of the cost function (10).

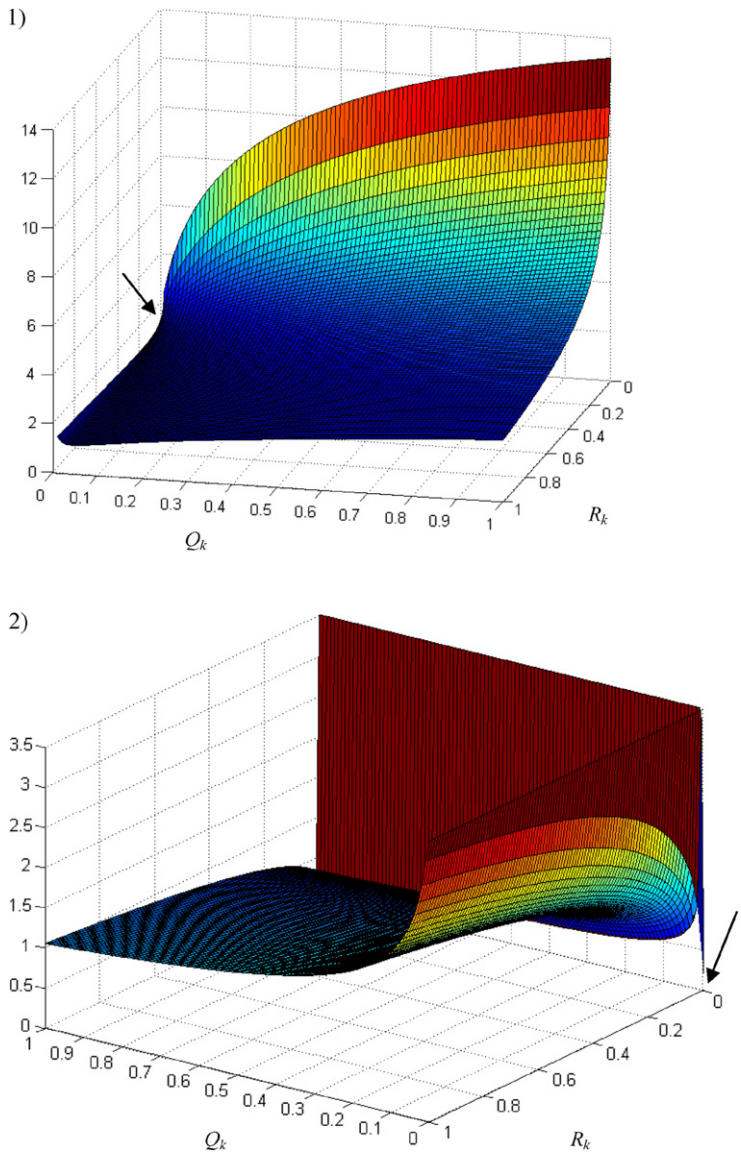

Fig. 8. The 3D plot of the cost function (the range of R_k and Q_k values is 0–1) for: 1) the acceleration, 2) the angular rate; arrows point at minima.

Table 2
Values of R_k and Q_k covariances received from optimization method.

	Accelerometer ADXL330	Gyroscope ADXRS300
R_k	5.8631×10^{-13}	1.9148×10^{-10}
Q_k	1.3458×10^{-11}	1.9674×10^{-7}

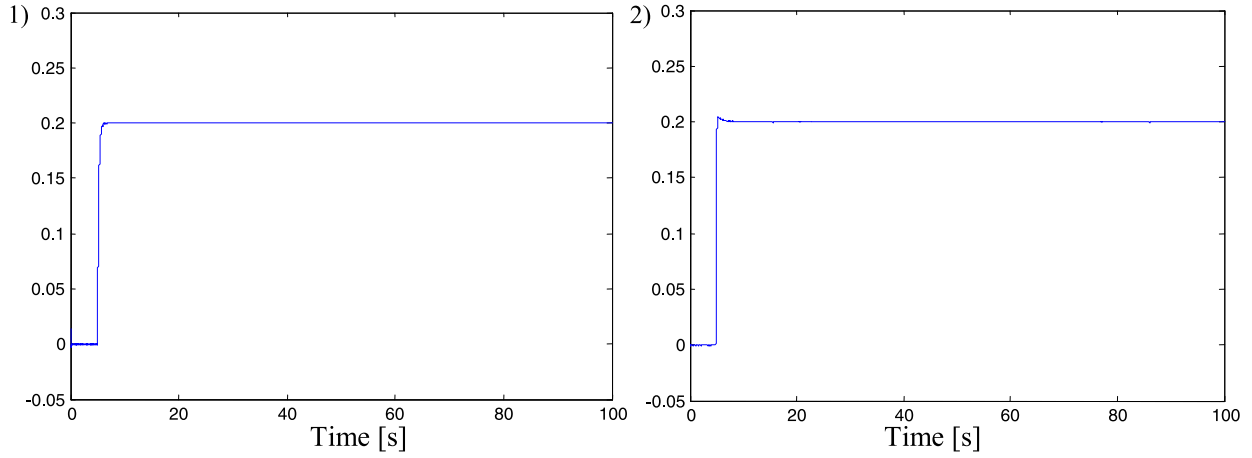

Fig. 9. KF responses for the step input signal in the case of: 1) acceleration, 2) angular rate. The optimal values of R_k and Q_k were taken from Table 2 ($P_0 = [11; 11]$).

where:

$S(\tau)$ – the step signal with initial value 0 and step of 0.2 at $t_s =$ 5th s,
$\hat{x}(\tau, R_k, Q_k)$ – the KF output signal while the input signal is: $z(\tau) = x(\tau) + S(\tau)$,
$x(\tau)$ – the measured signal of acceleration or angular rate,
F_S – the sampling frequency (10 [kHz]),
$\hat{X}(f, R_k, Q_k)$ – the Welch spectra of the KF output signal,
t_f – the time when $\hat{x}(\tau, R_k, Q_k) \geqslant S(\tau)$.

The first integral appearing in the cost function (10) is square of difference between the KF output signal and the step signal $S(\tau)$ while $t_s \leqslant \tau \leqslant t_f$ and it is responsible for minimizing the inertia of KF response. The second integral is an area below the curve of the Welch spectra and it is proportionally related to the noise level. The cost function (10) is realized as a Matlab script which also cooperates with a Simulink model shown in Fig. 7.

The graphic representation of the cost function (10) is presented in Fig. 8 as 3D plots separately for the acceleration and the angular rate. Arrows in the figure point at minima of the cost function.

Minimization of the cost function (10) using built-in Matlab function *fminsearch* results in the optimal values of R_k and Q_k (Table 2).

The KF response, while the input signal is $z(\tau) = x(\tau) + S(\tau)$ and KF parameters are fixed with optimal values of R_k and Q_k from Table 2, is shown in Fig. 9 for acceleration and angular rate signals separately. As we can notice in the figure the aim of the investigations was fully achieved. We are succeeded in finding of the optimal values of KF parameters which are suitable to use KF in our application. The optimal values of KF parameters satisfy both criterions of signal filtration quality: low noise level and high KF response rate. The success of the investigation was verified by KF behavior in the real-time filtering application performed as a routine of DSP processor. We observed constant and noiseless signals of acceleration and angular rate for the motionless measurement head and simultaneously any slight motion results in rapid signals change. So our KFs ensure good signal filtering without loss of sensitivity of the measurement head which was noticed earlier for parameters from Table 1.

5. Conclusions

The object movement is presented by signals of acceleration and angular rate containing additional random disturbances with characteristics of white Gaussian noise. A filtration of these signals is an important part of the strapdown system software and it impacts on the computation precision of the object position and orientation. Though all sensors of built measurement head have capacitors applied as low-pass filters of the output signals, the signals of acceleration and angular rate are still noised. So the problem is how to design Kalman filter, which could be used in the real-time filtering application, while the measurement noise covariance matrix is not known just as the measurement accuracy. To do this the main

attention was concentrated on the problem of the adjusting of KF parameters. Received results showed some difficulties to find appropriate parameter values because KF parameters, i.e. R_k, Q_k, and P_0 effect not only noises, but also modify the KF dynamics by the increase of the inertia in estimated signals. It is appeared that the best way to obtain optimal parameters is to use an optimization method. So the particular cost function was formulated. The final results of signals' filtering prove that the aim of investigation was achieved and designed Kalman filters are suitable to use them in the real-time applications for both signals of acceleration and angular rate. Designed KFs assure best signal filtering and high sensitivity of the measurement head.

References

[1] A. Ortyl, Z. Gosiewski, Strapdown inertial navigation system, Part 1. Navigation equations, J. Theor. Appl. Mech. 36 (1) (1998) 81–95.
[2] A. Lawrence, Modern Inertial Technology: Guidance and Control, Springer, 1998.
[3] D.H. Titterton, J.L. Weston, Strapdown Inertial Navigation Technology, Progress in Astronautics and Aeronautics, AIAA, Reston, 2004.
[4] Z. Gosiewski, A. Ortyl, Strapdown inertial navigation system, Part 2. Error equations, J. Theor. Appl. Mech. 36 (4) (1998) 937–962.
[5] P. Zarchan, H. Musoff, Fundamentals of Kalman Filtering: A Practical Approach, Progress in Astronautics and Aeronautics, AIAA, Reston, 2005.
[6] A.H. Mohamed, K.P. Schwarz, Adaptive Kalman filter for INS/GPS, J. Geodesy 73 (1999) 193–203.
[7] J. Wang, M.P. Stewart, M. Tsakiri, Adaptive Kalman filtering for integration of GPS with GLONASS and INS, IUGG/IAG, Birmingham, 1999.
[8] S.-T. Zhang, X.-Y. Wei, Fuzzy adaptive Kalman filtering for DR/GPS, in: Proc. of the Second International Conference on Machine Learning and Cybernetics, Xi'an, 2003, pp. 2634–2637.
[9] Dah-Jing Jwo, Shun-Chieh Chang, Application of optimization technique for GPS navigation Kalman filter adaptation, in: ICIC (1), 2008, p. 227.
[10] ADXL300, Small, Low Power, 3-Axis ±3 g iMEMS® Accelerometer, Analog Devices.
[11] ADXRS300, ±300°/s Single Chip Yaw Rate Gyro with Signal Conditioning, Analog Devices.
[12] J.R. Huddle, Inertial navigation system error-model consideration in Kalman filtering application, Control Dyn. Syst. 20 (1983) 293–338.
[13] P.S. Maybeck, Advances applications of Kalman filters and nonlinear estimations in aerospace systems, Adv. Control Dyn. Syst. 20 (1983) 67–154.
[14] W. Lechner, Application of model switching and adaptive Kalman filtering for aided strapdown navigation system, Adv. Control Dyn. Syst. 20 (1983), Part 2.
[15] S. Konatowski, A. Pieniężny, Estimation of UAV position by nonlinear Kalman filters, Zeszyty Naukowe Politechniki Rzeszowskiej. Mechanika 71 (238) (2007) 317–324.

Cezary Kownacki is an Adjunct Assistant Professor at the Faculty of Automation and Robotics in the Department of Mechanical Engineering of Bialystok Technical University. He received a Ph.D. in Mechanical Engineering and Signal Processing from Bialystok Technical University (BTU) in 2005, an M.Eng. in Automation and Robotics from BTU in 1998. Cezary's research interests include autonomous mobile robots, micro air vehicles, navigation algorithms and IMU signals processing.